J Solid State Electrochem (2017) 21:649–656
DOI 10.1007/s10008-016-3411-4

ORIGINAL PAPER

Cobalt oxyhydroxide/graphene oxide nanocomposite for amelioration of electrochemical performance of lithium/sulfur batteries

Seyyed Taher Seyyedin[1] · **Mohammad Reza Yaftian**[1] · **Mohammad Reza Sovizi**[2]

Received: 16 May 2015 / Revised: 29 February 2016 / Accepted: 25 September 2016 / Published online: 1 October 2016

Abstract Cobalt oxyhydroxide combination with graphene oxide (CoOOH@GO) as a novel conductive matrix is developed for high performance lithium/sulfur batteries. Enhancement retention of polysulfide species into matrix of cobalt oxyhydroxide anchored on graphene oxide flakes by strong chemical binding of carbon-sulfur is demonstrated. Sulfur incorporated in the sheet-like morphology of CoOOH@GO delivers high initial discharge specific capacity of 1190.85 mAh/g, which raises 260 mAh/g with respect to graphene oxide/sulfur (GO/S) as a cathode material. Furthermore, CoOOH@GO/S maintains the average coulombic efficiency of 96 % after 300 cycles at 1 C rate with capacity retention of about 61 %. Good current rate capability of CoOOH@GO/S cathode reveals that the resulting composite is open platform for electrolyte diffusion and fast ion transportation leading to the improved electrochemical performance of lithium/sulfur batteries.

Keywords Lithium/sulfur battery · Sheet like structures · Metal oxyhydroxide · Sulfur cathode

Introduction

The necessity of energy resources producing high energy density and inflicting least damages to environment and climate changes has significantly increased. Although lithium ion batteries meet many advantages in generating and storing energy, and have proven successful in the portable electronics market, due to their low energy density, they cannot still provide current requirements of electrical and hybrid machines and large-scale energy storage [1–4].

In recent years, lithium/sulfur batteries have attracted much attention because of their high potentiality in creating 2–3 times more energy density (2600 Wh/kg) and about 5 times more theoretical capacity (1672 mAh/g) in comparison with common traditional lithium ion batteries. Lithium/sulfur batteries have been introduced as a new generation of rechargeable lithium batteries [5, 6]. These batteries bear some advantages including low cost, abundant, non-toxic, and environment-friendly. Furthermore, lithium/sulfur batteries are able to provide requirements of energy storage systems for renewable energy resources and produce high energy density for automobile industry [7]. Despite these advantages, there are some problems which shorten the practical lifespan of these batteries. Low electrical conductivity of active material and high volume expansion are among the deficiencies of these types of batteries [8–10]. In addition, high solubility of polysulfide into the electrolyte, which cause the precipitation on the anode surface in discharging process, and then on the cathode surface during the charging process (shuttle effect), limit their efficiency. It results in reduction of the active substance of sulfur, declining of coulombic efficiency and capacity fading during first cycles [11]. These problems have prohibited the commercialization of lithium/sulfur batteries.

Graphene, an allotrope of carbon, is also an appropriate choice to achieve the required electrical conductance and diminishing the polysulfide diffusion into the electrolyte [12]. It has high surface area (over 2600 m^2/g), good chemical and mechanical stability, suitability, and flexibility [13]. Various modified graphene such as graphene oxide [14–16],

✉ Mohammad Reza Yaftian
yaftian@znu.ac.ir

[1] Phase Equilibria Research Laboratory, Department of Chemistry, Faculty of Science, University of Zanjan, Zanjan 45371-38791, Iran

[2] Faculty of Chemistry and Chemical Engineering, Malek Ashtar University of Technology, P.O. Box 16765-3345, Tehran, Iran

coating graphene/sulfur composite [17, 18], doping with nitrogen [19] and hybrid structures [20, 21] have been studied for providing stronger chemical bond C-S to trap polysulfides into the matrix. Recently, the superior interactions of metal oxides-polysulfides have been proved [22, 23]. Metal oxides, such as TiO_2 [24], Ti_4O_7 [25], Al_2O_3 [26], La_2O_3 [27], and Co $(OH)_2$ [28] have demonstrated high affinity for polysulfide maintenance to hinder the diffusion of the soluble intermediates.

In this paper, we report a simple method to prepare sulfur confined into the layers of graphene oxide (GO) anchored with cobalt oxyhydroxide (CoOOH) sheets as a cathode. Because of the strong chemical bonding of carbon-sulfur CoOOH@GO/S in comparison with graphene oxide/sulfur nanocomposite, the electrochemical performance of the conductive matrix of lithium/sulfur cells is highly improved. It was assumed that CoOOH@GO sheets have effective specific surface area to incorporate sulfur homogeneously with strong chemical and physical interactions. To the best of our knowledge, this report is the first work on the application of metal oxyhydroxide@GO composites for modification of cathodes in lithium/sulfur batteries.

Experimental

Chemicals

Natural graphite (Aldrich), hydrogene peroxide (30 wt%), potassium permanganate, hexahydrated cobalt nitrate, potassium hydroxide, sulfur, sulfuric acid, hydrochloride acid (Merck), cetyltributylammonium bromide (CTAB), dimethyl sulfoxide (DMSO), polyvinyldifluoride (PVdF), *N*-methyl-2-pyrrolidone (NMP), lithium bis(trifluoromethanesulfone)imide (LiTFSI), 1,3-dioxolane (DOL), poly(ethylene glycol) dimethyl ether (PEGDME), polyethylene (Celgard 2400) (Sigma-Aldrich), and carbon black (Akzo Nobel) were used. Ultrapure water was used in all experiments.

Apparatus

The morphologies of materials were analyzed by field emission scanning electron microscopy (Tescan, Mira3) operating at 20 kV coupled to an energy dispersive X-ray spectrometer (EDS). The powder X-ray diffraction (Bruker AXS, D8 advance diffractometer) and X-ray photoelectron spectroscopy (XPS, VG Microtech, Twin anode, XR3E2 X-ray source, using Al K_ = 1486.6 eV) measurements were performed to characterize materials structure. Elemental analysis (Analytica Jena, multi EA-3100) was performed for measurement of sulfur in the synthesized CoOOH@GO/S and GO/S. The amount of sulfur was determined to be ~52 % and ~54 % in the CoOOH@GO/S and GO/S composites, respectively. The electrochemical properties of the CoOOH@GO/S composite cathode was tested by galvanostatic discharge and charge (Kimiapardaz Iran, Kimiastat 126) in a potential range of 1.5–3.0 V (vs. Li/Li+). Cyclic voltammetry (CV) measurements were performed in the potential range 1.5–3.2 V (vs. Li/Li+) at a scan rate of 0.1 mVS-1 by using an electrochemical workstation (Biologic, VSP 300). Electrochemical impedance spectrum (EIS) measurements was determined using a frequency response analyzer (Biologic, VSP 300) in the frequency range 0.01 Hz to 100 kHz at potentiostatic signal amplitude of 5 mV.

Preparation of CoOOH@GO/S

Preparation of graphene oxide sheets

Modified Hummer's method was used to prepare GO sheets [29]. Graphite powder (2 g) was stirred with 46 mL concentrated sulfuric acid for 8 h. Then, potassium permanganate (6 g) was added gradually and the mixture was stirred mechanically while the reaction vessel was put in an ice bath. The mixture was stirred at 35–40 °C for 30 min, and then for further 45 min at 70–75 °C. A portion of 92 mL of ultrapure water was slowly added into this mixture, and it was heated at 100–105 °C for 30 min. After an addition of 280 mL of ultrapure water and 20 mL hydrogen peroxide (30 %), the resulted suspension was washed repeatedly with 15 mL diluted solution of hydrochloric acid (5 %), until the barium ion test confirmed the elimination of the sulfate ion. Finally, the product (GO sheets) was dried in vacuum at 60 °C overnight.

Preparation of CoOOH@GO nanocomposite

The CoOOH@GO nanocomposite was synthesized through a sonochemical assisted precipitation followed by thermal treatment. The typical route is as follows. In the first step, 2.416 g of cobalt nitrate hexahydrate was dissolved in ultrapure water (50 mL) with vigorous stirring at room temperature. Then 10 mg of dispersed GO sheets in 10 mL of ultrapure water was dropped into the solution of cobalt nitrate under ultrasonic irradiation for 1 h. A volume of 50 mL of potassium hydroxide solution (1 mol L^{-1}) was added dropwise to the mixture. Subsequently, it was ultrasonicated for further 1 h. This mixture was heated at 80 °C for 30 min. The obtained black product was washed with ultrapure water several times and was dried at 60 °C overnight.

Preparation of CoOOH@GO/S

As reported by [30, 31], process of dissolving sulfur in DMSO at 90 °C is an appropriated method for producing sulfur nanoparticles. A modified procedure was used for a better deposition of sulfur. Sulfur nanoparticles can penetrate inter layers of

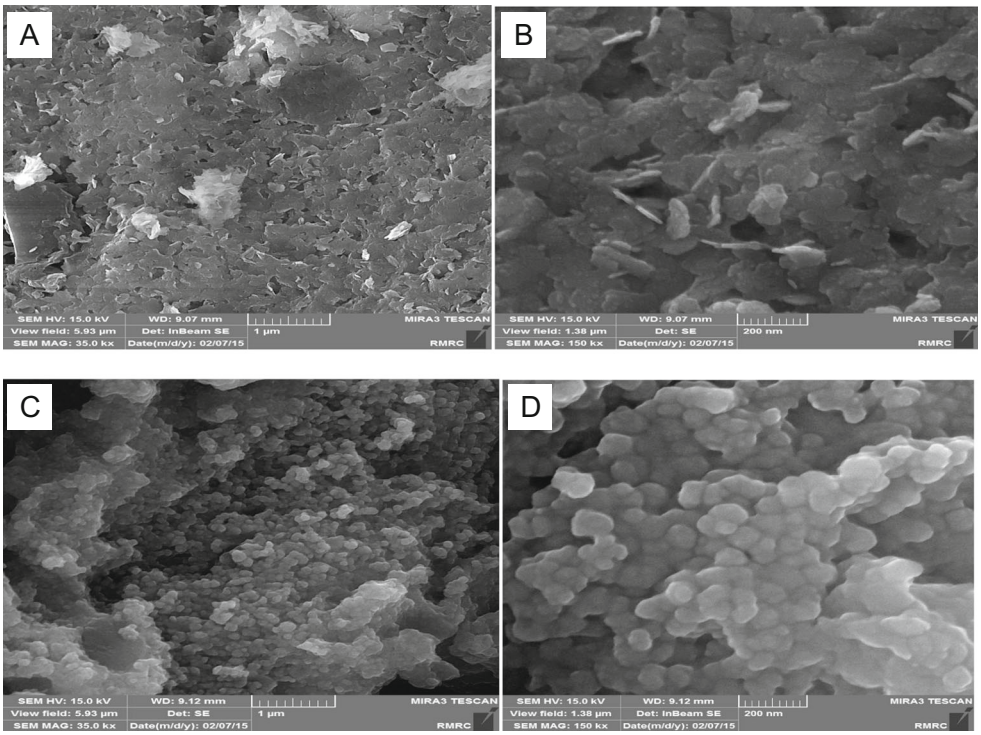

Fig. 1 Low and high magnification SEM images of the CoOOH@GO nanosheets (**a**, **b**) and CoOOH@GO/S nanocomposite (**c**, **d**)

CoOOH@GO matrix. The presence of water as anti-solvent helps to infiltrate sulfur insides of the host material. The application of CTAB surfactant allowed a suitable mingling of the phases. In order to, a total of 1.5 g CoOOH@GO was well dispersed in 100 mL of water. An amount of 1.8 g of sulfur was dissolved in the solution of dispersed CoOOH@GO. The temperature of resulted suspension was kept at 90 °C. To this mixture was added 0.01 g CTAB and 40 mL of DMSO. After about 20 min, the mixture was moved to autoclave under argon atmosphere at 90 °C. After 5 h, the obtained product (CoOOH@GO/S) was collected by centrifugation and then washed with ultrapure water.

Cathode preparation

The cathode consisted of 80 wt% as-prepared CoOOH@GO/S nanocomposite, 10 wt% polyvinylidene fluoride (PVDF) binder, and 10 wt% carbon black. The mixture was mixed

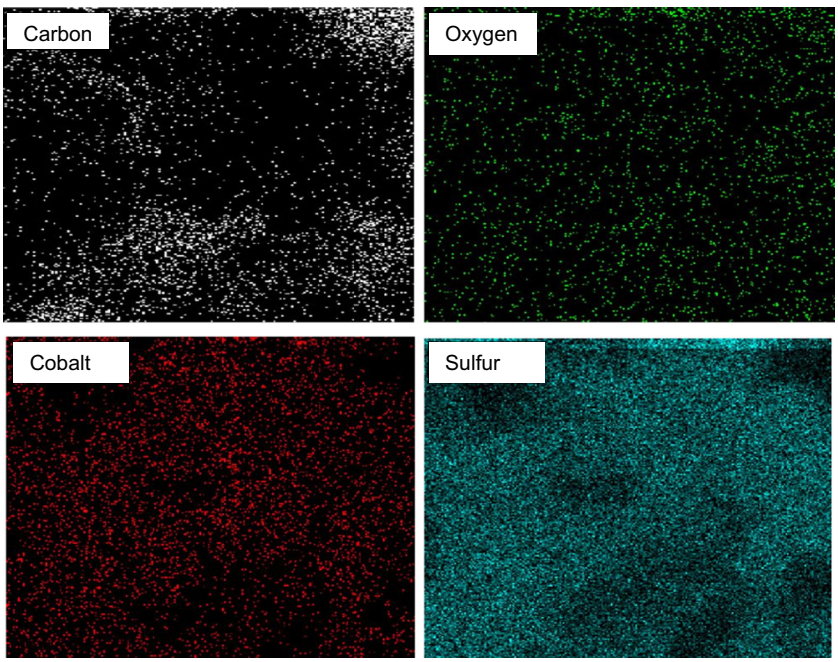

Fig. 2 Elemental mapping of carbon, oxygen, cobalt, and sulfur in CoOOH@GO/S nanocomposite

and dipersed in *N*-methyl-2-pyrrolidone (NMP) to form a slurry which was then speared to an aluminum foil substrate with an average sulfur loading of 2 mg/cm^2 and dried at 70 °C for 2 h. A 2032- type coin cell was assembled in an argon filled glove box using CoOOH@GO/S based cathode, lithium foil as the anode, and porous polyethylene (Celgard 2400) film as separator. The electrolyte was 1 mol L^{-1} lithium bis(trifluoromethanesulfone)imide (LiTFSI) in a mixed solvent of 1,3-dioxolane (DOL) and poly(ethylene glycol) dimethyl ether (PEGDME) (1:1 volume ratio).

Results and discussion

Scanning electron microscopy (SEM) was used to examine the morphology and surface structure of the adsorbent at the required magnification at room temperature. The morphology of the synthesized CoOOH@GO and CoOOH@GO/S nanocomposites was characterized by SEM images (Fig. 1). It is found that the surfaces of GO flakes are uniformally decorated by cobalt oxyhydroxide nanosheets, forming the CoOOH@GO nanocomposite without any agglomeration. It is estimated that the thickness of cobalt oxyhydroxide sheets is about 15–20 nm. After absorption of sulfur nanoparticles into the nanosheets, no apparent bulk sulfur can be observed on the CoOOH@GO/S surface. As expected, the surface morphology has been changed by applying hydrothermal condition during sulfur infiltration [32].

Elemental mapping of carbon, oxygen, cobalt, and sulfur in the structure of CoOOH@GO/S are acquired with the energy-dispersive X-ray (EDX) microanalysis. As displayed in Fig. 2, these elements are homogenously dispersed in the CoOOH@GO/S structure. Clearly it is seen that S nanoparticles are uniformly distributed in the synthesized conductive matrix. As it is shown in Fig. 2, carbon mapping is not uniformly distributed. This can be attributed to the application of carbon glue, for a better stabilization of the sample, during the preparation of sample for SEM analysis. The contribution of this extra carbon, makes an ununiformly distribution of the carbon map.

Figure 3 contains the XRD patterns of CoOOH@GO and CoOOH@GO/S nanocomposites. The pattern of cobalt oxyhydroxide graphene oxide shows the refraction peaks that can be indexed to a rhombohedral structure. The diffraction peaks are in good agreement with uniformly decorating of graphene oxide flakes by CoOOH sheets (JCPDS No.07–0169). The XRD pattern of CoOOH@GO/S nanocomposite has peaks similar to those of CoOOH@GO, including the obvious incorporation of sulfur into CoOOH@GO host matrix. (XRD pattern of pure sulfur (JCPDS No. 01–077–0145) is presented in Fig. 3).

It is well-known that the GO nanocomposite has their planes decorated frequently with epoxy, hydroxyl, carbonyl, and carboxyl groups [18]. In appearance of CoOOH as Lewis acid, breaking C-O bonds (especially epoxy groups) have increased and form much C-S bonds afford the confinement of nanosulfur attaching into the CoOOH@GO sheets [33]. After sulfur immobilization, thin layer of CoOOH with a thickness of tens of nanometers is distributed uniformly on the GO sheets with no significant particles of bulk sulfur depicted on the external surface of the CoOOH@GO/S. The sheets seem form a two-dimensional network nanostructure, which increases surface area and the efficient liquid-solid interfacial area that can significantly absorb sulfur particles, thereby affects the performance of lithium/sulfur batteries.

Figure 4 displays discharge profile at 0.1 current rate of the lithium/sulfur batteries with the GO/S and CoOOH@GO/S cathodes. Both discharge curves have two-voltage plateaus. It is seen that significant differences exist between the two

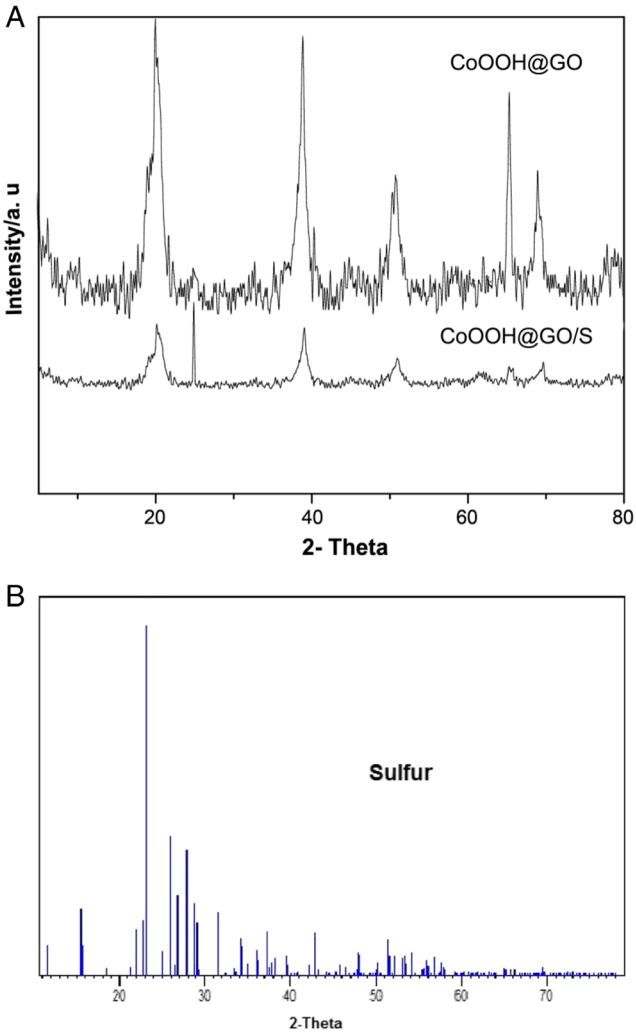

Fig. 3 XRD patterns of CoOOH@GO and CoOOH@GO/S nanocomposites and pure sulfur pattern

discharge plateaus. The GO/S discharge plateau is relatively shorter while discharge capacity of CoOOH@GO/S cathode is extended about 260 mAh/g longer. This confirms strong interactions between matrix with polysulfide intermediates through epoxides ring opening of cobalt oxyhydroxide.

The CoOOH may contribute in improved specific capacity of CoOOH@GO/S composite. Thus, the evaluating electrochemical performance of species is important. Figure 5 shows cyclic voltammetry (CV) curves of a lithium/sulfur cell with the pure CoOOH, GO/S, and CoOOH@GO/S cathodes, obtained at a scan rate of 0.1 mV S^{-1} and potential range of 1.5–3.2 V vs. Li/Li^+. The cyclic voltammetry of pure CoOOH has shown that there is not any significant current in applied voltage range of Li/S cell. This allowed conclusion that the contribution of CoOOH in improved specific discharge capacity is negligible. As shown in second cycle of GO/S nanocomposite and second and third cycles of CoOOH@GO/S composite, two well-defined cathodic peaks are observed. These peaks correspond to the multistep reaction mechanism of elemental sulfur with lithium ions [34, 35]. The cathodic peak centered about 2.40 V is assigned to the reduction of the S_8 ring to higher polysulfide (Li_2S_n, $2 < n < 8$). The reduction peak at 1.96 V is a subsequent reduction to Li_2S_2 and eventually to Li_2S. In the anodic sweep, an oxidation peak at 2.4 V with a shoulder at about 2.55 V, attributes to reversely transformation of Li_2S_2/Li_2S and high order polysulfides to sulfur during the charging process [35]. In comparison with GO/S, the cathodic peaks of CoOOH@GO/S have shifted to higher potentials, and the anodic peak has shifted to lower potentials, which suggest good reversible transitions that can be taken place from higher order polysulfides to Li_2S during the discharge/charge processes.

Figure 6a displays the corresponding discharge/charge curves of the CoOOH@GO/S composite material at different current rates (current rate was on the theoretical specific capacity of sulfur, where a 1 C has current density of ~1675 mA/g) in the potential range of 1.5–3.0 V vs. Li/Li^+.

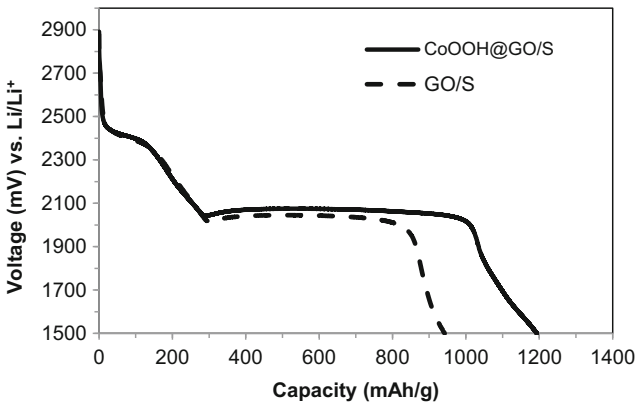

Fig. 4 Discharge profiles at 0.1 C-rate of lithium/sulfur cells with GO/S and CoOOH-GO/S cathodes

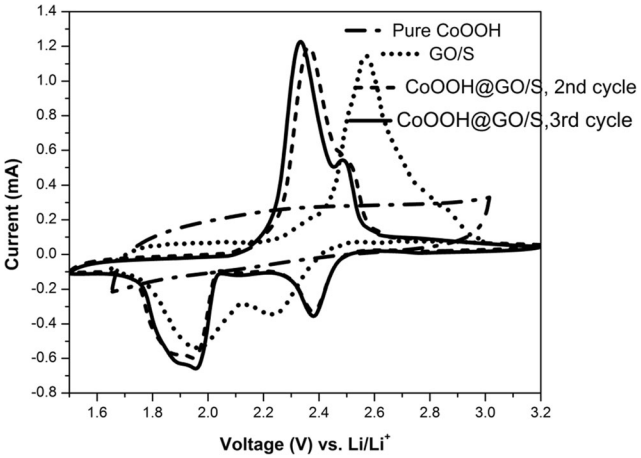

Fig. 5 Cyclic voltammetry curves of the pure CoOOH, GO/S, and CoOOH-GO/S cathodes in the potential range from 1.5 to 3.2 V (vs. Li/Li^+) at the scan rate of 0.1 mVS^{-1}

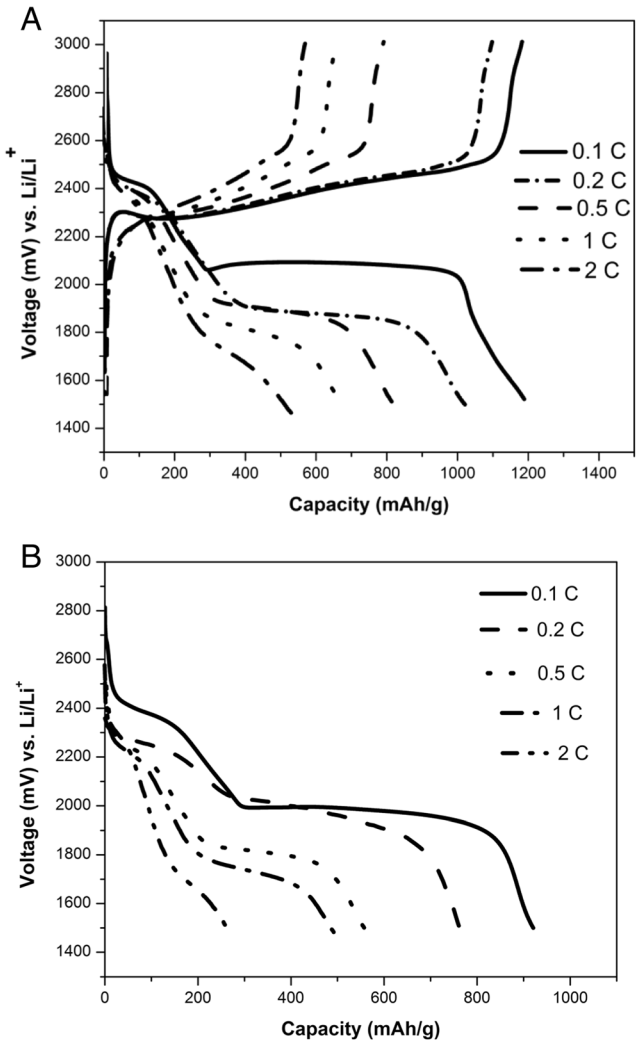

Fig. 6 Voltage-capacity profiles of CoOOH@GO/S electrode at different discharge/charge current rates (**a**) Voltage-capacity profiles of GO/S composite (**b**)

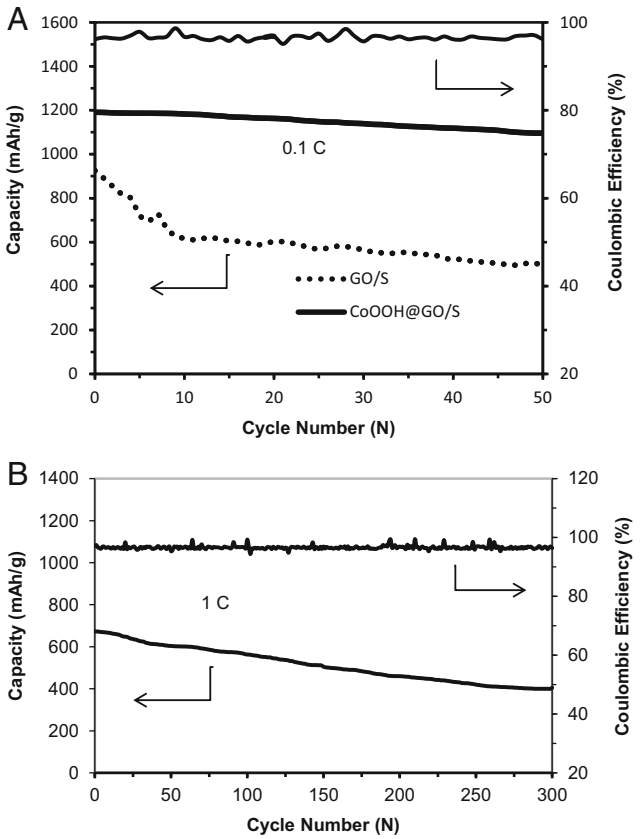

Fig. 7 Cycling performance of GO/S and CoOOH@GO/S electrodes at 0.1 C (**a**) Cycling performance of CoOOH@GO/S composite at 1 C (**b**)

The discharge profiles of all current densities were obtained by a two-plateau behavior as reported for the S cathode [36], which are coordinated to the formation of higher order polysulfides (Li_2S_n, $4 \leq n \leq 8$) at the first plateau and lower orders Li_2S_2/Li_2S at the second plateau. It has shown that both the discharge voltage plateau and the discharge capacity decline significantly with growing current rate. This can be attributed to the increasing overvoltages of kinetic and ohmic at higher current rate. For comparison, voltage-discharge capacity curves of GO/S nanocomposite are presented in Fig. 6b. The discharge profiles of all current densities were obtained by two plateaus as expected. The GO/S nanocomposite exhibits good rate performance, and specific capacities of 925.90, 784.74, 563.49, 498.17, and 261.18 mAh g^{-1} have obtained at 0.1, 0.2, 0.5, 1 and 2 C, respectively. The rate of capacity fading in the presence of cobalt species is lower than GO/S nanocomposite as the cathode. It corresponds to addition of cobalt oxyhydroxide in the electrode structure and increasing probability of C-S bond formation by breaking C-O bond with Lewis acid function of CoOOH.

Galvanostatic charge/discharge cycling is performed for studying the cycling performance of the CoOOH@GO/S and GO/S cathode materials. As depicted in Fig. 7, the cycling performance of the lithium/sulfur cells with active sulfur immobilized in CoOOH@GO and GO conductive matrixes are obtained at current rate of 0.1 C. The high initial discharge capacity of 1191.15 mAh g^{-1} in 0.1 C is obtained in the presence of cobalt species. The discharge capacity reduces to about 1096.14 mAh g^{-1} after 50 cycles, showing a capacity loss of 7.98 %. While, discharge capacity of GO/S is about 495.01 mAh g^{-1}after 50 cycle that shows capacity loss of

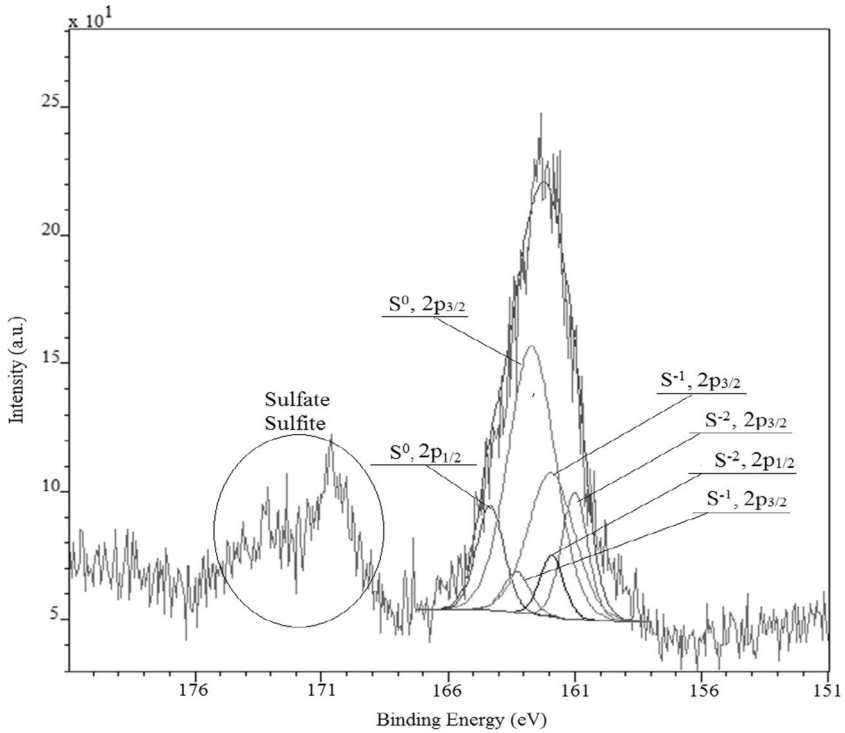

Fig. 8 XPS measurement of CoOOH@GO/S composite electrode. XP spectra of the S 2p core-level of the cathode

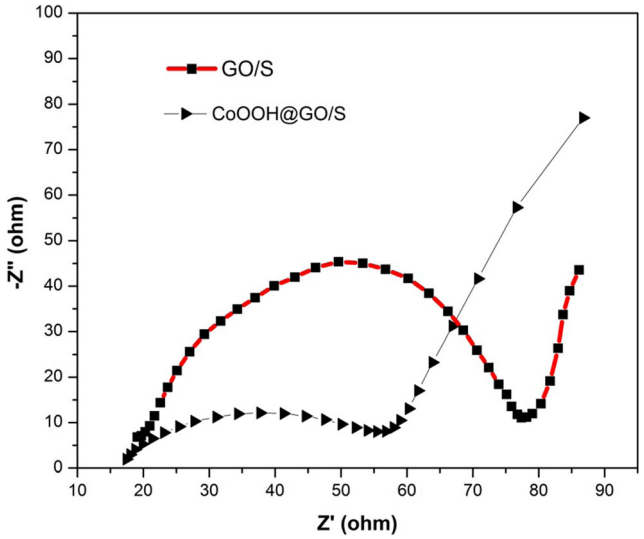

Fig. 9 Electrochemical impedance spectroscopy of the lithium/sulfur cells with CoOOH@GO/S and GO/S nanocomposites as cathode

46.4 %. Also, the Li/CoOOH@GO/S cell retained a good coulombic efficiency, with the average of about 96.5 % after 50 cycles. The results indicate positive presence of cobalt oxyhydroxide for the formation of much C-S chemical bond in comparison with interaction of pure graphene oxide flakes with sulfur during cycling. It makes significant improvement in cycle performance of Li/S cell at low rate. With the increase of current density rate to 1 C, CoOOH@GO/S cathode exhibits an initial discharge capacity of about 673.1 mAh g^{-1}. After 150 cycles, this capacity declined to about 505 mAh g^{-1} with a capacity loss of 25 %. After 300 cycles, the cell still maintain a reversible discharge capacity of 405.1 mAh g^{-1}, representing a capacity retention of 61 %. The average Coulombic efficiency of the cell at 1 C was still above 96 %. It is proven that because of Lewis acid acting of CoOOH, strong chemical bonds of C-S are increased in the conductive matrix of CoOOH@GO/S. Also, effective surface area for wrapping nanosulfur to trap polysulfide species physically into the conductive matrix can help electrolyte access whole of the structure, and provide buffering space for volume expansion of sulfur during discharge/charge at higher rates.

It is important to know the reduced graphene oxide could exhibit higher electronic/ionic conductivities with superior flexibility and porosity, but because of special properties of CoOOH, and GO are selected for this work. The CoOOH species can be considered as Lewis acid for accelerating C-S bond formation by breaking C-O bond of epoxy groups of graphene oxide. So, the number C-S chemical bond is increased in CoOOH@GO/S nanocomposite with respect to GO/S composite. In order to understand the function of CoOOH during charging and discharging reactions of Li-S battery, XPS measurement was performed after the fifty cycles (charge state). As shown in Fig. 8, the deconvolution of the S 2p core level XPS of CoOOH@GO/S nanocomposite leads to six peaks, resulting from different electronic states. The electrode of the cell exhibited three components in the S 2p XP spectrum, associated to a Li_2S_2, Li_2S, and neutral sulfur. The peaks corresponding to sulfide species (Li_2S_2 and Li_2S) with a substantial loss in intensity proves presence of unreacted Li_2S and Li_2S_2 even after complete charge could be responsible for irreversible capacity loss during charge and discharge. It is important to note the Li_2S_2 peak is growing at the same binding energy attributed to carbon-sulfur interaction [37]. From the XPS results, it has postulated that the chemical bond formation of C-S assists in the nucleation and formation of Li_2S_2 and Li_2S, and address higher polysulfides intermediate diffusion into the electrolyte. Further, in the presence of CoOOH species, because of increasing formation of C-S interaction, improved electrochemical performance is possible.

A further evidence for the high electrical conductivity of the cell with prepared CoOOH@GO/S cathode in comparison with that contains GO/S cathode, electrochemical impedance spectroscopy (EIS) is attained (Fig. 9). It is obvious that the charge transfer resistance of the cell with CoOOH@GO/S electrode is lower than preparing and constructing with GO/S. This can be attributed to the modification of functional groups on the graphene oxide (GO), and the presence of nanosized CoOOH sheets in the layers of graphene oxide flakes to prevent from stacking [38], that certify a fast electron transfer, which considerably helps to the rate performance of the lithium/sulfur cell with CoOOH@GO/S as a cathode.

Conclusion

In summary, we have designed graphene oxide coated with cobalt oxyhydroxide (CoOOH@GO) for wrapping of sulfur nanoparticles in conductive matrix. Homogenous coated of sheet-like morphology CoOOH in layers of graphene oxide flakes and epoxides opening ring property of cobalt species provide an effective surface area to decrease polysulfides shuttling that causes improvement of specific discharge capacity in comparison with GO/S cathode. Indeed, the strong chemical binding between C-S in CoOOH@GO/S and open environment of this nanocomposite have provided the perfect opportunity to absorb intermediate polysulfides generated in discharge reaction, and accommodate volume expansion during charge/discharge fast ion transportation. We have showed that Li/S cell with this cathode delivers 61 % of initial reversible discharge capacity after 300 charge/discharge cycles at 1 C rate, with an average coulombic efficiency of 96.15 %. We hope this architecture of graphene oxide and cobalt oxyhydroxide can open a new insight to design novel concept of carbonaceous material and transition metal oxides/hydroxides for improving performance of high energy density lithium/sulfur batteries.

References

1. Cairns EJ, Albertus PA (2010) Rev Chem Biomol Eng 1:299–320
2. Armand M, Tarascon JM (2008) Nature 451:652–657
3. Whittingham MS (2008) MRS Bull 33:411–419
4. Goodenough JB, Kim Y (2010) Chem Mater 22:587–603
5. Chen M, Adams S (2015) J Solid State Electrochem 19:697–702
6. Li X, Lushington A, Liu J, Li R, Sun X (2014) Chem Commun 50: 9757–9760
7. Ji X, Nazar LF (2010) J Mater Chem 20:9821–9826
8. Huang C, Xiao J, Shao YY, Zheng JM, Bennett WD, Lu DP, Laxmikant SV, Engelhard M, Ji LW, Zhang J, Li XL, Graff GL, Liu J (2014) Nat Commun 5:3015–3023
9. Geng X, Rao M, Li X, Li W (2013) J Solid State Electrochem 17: 987–992
10. Song MK, Cairns EJ, Zhang TG (2013) Nanoscale 5:2186–2204
11. Mikhaylik YV, Akridge JR (2004) J Electrochem Soc 151:A1969–A1976
12. Evers S, Nazar LF (2012) Chem Commun 48:1233–1235
13. Geim AK (2009) Science 324:1530–1534
14. Ji L, Rao M, Zheng H, Zhang L, Li Y, Duan W, Guo J, Cairns EJ, Zhang Y (2011) J Am Chem Soc 133:18522–18525
15. Rong J, Ge M, Fang X, Zhou C (2014) Nano Lett 14:473–479
16. Hu G, Xu C, Sun Z, Wang S, Cheng HM, Li F, Ren W (2015) Adv Mater. doi:10.1002/adma.201504765
17. Wang H, Yang Y, Liang Y, Robinson JT, Li Y, Jackson A, Cui Y, Dai H (2011) Nano Lett 11:2644–2647
18. Zhou WD, Chen H, Yu YC, Wang D, Cui Z, DiSalvo FJ, Abruna HD (2013) ACS Nano 7:8801–8808
19. Qiu YC, Li WF, Zhao W, Li G, Hou Y, Liu M, Zhou L, Ye FM, Li HF, Wei ZH, Yang S, Duan WH, Ye Y, Guo JH, Zhang YG (2014) Nano Lett 14:4821–4827
20. Yang X, Zhang L, Zhang F, Huang Y, Chen YS (2014) ACS Nano 8:5208–53015
21. He G, Hart CJ, Liang X, Garsuch A, Nazar LF (2014) Appl Mater Interfaces 6:10917–10923
22. Liang X, CY Kwok, FL Marzano, Q Pang, M Cuisinier, H Huang, CJ Hart, D Houtarde, Kaup K, Sommer H, Berezesinski T, Janek J, LF Nazar (2015) Adv Energy Mater 1501636. doi:10.1002/aenm.201501636
23. Ji X, Evers S, Black R, Nazar LF (2011) Nat Commun 2:325–331
24. She ZW, Li WY, Cha JJ, Zheng GY, Yang Y, McDowell MT, Hsu PC, Cui Y (2013) Nat Commun 4:1331–1337
25. Tao X, Wang J, Ying Z, Cai Q, Zheng G, Gan Y, Huang H, Xia Y, Liang C, Zhang W, Cui Y (2014) Nano Lett 14:5288–5294
26. Dong K, Wang SP, Zhang HY, Wu JP (2013) Mater Res Bull 48: 2079–2083
27. Sun FG, Wang JT, Long DH, Qiao WM, Ling LC, Lv CX, Cai R (2013) J Mater Chem 1:13283–13289
28. Niu XQ, Wang XL, Wang DH, Li Y, Zhang YJ, Zhang YD, Yang T, Yu T, Tu JP (2015) J Mater Chem A 3:17106–17112
29. Hu J, Dong YL, Chen XJ, Zhang HJ, Zheng JM, Wang Q, Chen XG (2014) Chem Eng J 236:1–8
30. Li K, Wang B, Su D, Park J, Ahn H, Wang G (2012) J Power Sources 202:389–393
31. Ryu HS, Park JW, Park J, Ahn JP, Kim KW, Nam TH, Wang G, Ahn HJ (2013) J Matter Chem A 1:1573–1578
32. Liu L, Xu X (2015) SpringerPlus 4:732–741
33. Bardoloi A, Hwang YK, Hwang JS, Halligudi SB (2009) Catalysis Communication 10:1398–1403
34. Ji X, Lee KT, Nazar LF (2009) Nat Mater 8:500–506
35. Jeddi K, Sarikhani K, Mahmoudreza Ghaznavi M, Zendehboodi S, Chen P (2015) J Solid State Electrochem 19:1161–1169
36. Wang HL, Yang Y, Liang YY, Robinson JT, Li YG, Jackson A, Cui Y, Dai HJ (2011) Nano Lett 11:2644–2647
37. Helen M, Reddy MA, Diemant T, Schindeler UG, Behm RJ, Kaiser U, Fichtner M (2015) Sci Rep 5:12146–11261
38. Chen YL, Hu ZA, Chang YQ, Wang HW, Zhang ZY, Yang YY, Wu HY (2011) J Phys Chem C 115:2563–2571